

**PROCESSING AND DAMAGE TOLERANCE OF CONTINUOUS CARBON FIBER COMPOSITES  
CONTAINING PUNCTURE SELF-HEALING THERMOPLASTIC MATRIX**

Brian W. Grimsley, Keith L. Gordon, Michael W. Czabaj, Roberto J. Cano, and Emilie J. Siochi

NASA Langley Research Center Hampton, VA 23681

**ABSTRACT**

Research at NASA Langley Research Center (NASA LaRC) has identified several commercially available thermoplastic polymers that self-heal after ballistic impact and through-penetration. One of these resins, polybutadiene graft copolymer (PBg), was processed with unsized IM7 carbon fibers to fabricate reinforced composite material for further evaluation. Temperature dependent characteristics, such as the degradation point, glass transition ( $T_g$ ), and viscosity of the PBg polymer were characterized by thermogravimetric analysis (TGA), differential scanning calorimetry (DSC), and dynamic parallel plate rheology. The PBg resin was processed into  $\approx 22.0$  cm wide unidirectional prepreg tape in the NASA LaRC Advanced Composites Processing Research Laboratory. Data from polymer thermal characterization guided the determination of a processing cycle used to fabricate quasi-isotropic 32-ply laminate panels in various dimensions up to 30.5cm x 30.5cm in a vacuum press. The consolidation quality of these panels was analyzed by optical microscopy and acid digestion. The process cycle was further optimized based on these results and quasi-isotropic, [45/0/-45/90]\_S, 15.24cm x 15.24cm laminate panels were fabricated for mechanical property characterization. The compression strength after impact (CAI) of the IM7/pBG composites was measured both before and after an elevated temperature and pressure healing cycle. The results of the processing development effort of this composite material as well as the results of the mechanical property characterization are presented in this paper.

**1. INTRODUCTION**

The initiation and propagation of damage ultimately results in failure of aircraft structural components. Often, impact damage is difficult to identify in-service and hence design of continuous carbon fiber reinforced polymer (CFRP) composite structure involves up to a 50% knockdown in the undamaged failure strength allowable. If damage is identified in a composite structure, the vehicle must be grounded for structural repair. This involves the grinding away of damaged regions and drilled holes to secure patches. Any activity which disturbs the load bearing carbon fibers introduces new sites for damage initiation and accumulation, further weakening the structure [1]. By providing a polymer matrix with the ability to self-heal, after impact damage is incurred, greatly improves vehicle safety by increasing the design allowable for strength, resulting in more efficient CFRP structure. Self-healing polymeric materials have been defined in the literature as “materials which have the built in capability to substantially recover their load transferring ability after damage. Such recovery can occur autonomously or non-autonomously, in which case assisted healing is activated after an application of a specific stimulus (e.g. heat, radiation)” [2]. Effective self-healing requires that these materials heal quickly following low - mid velocity impacts, while retaining structural integrity. Although there are materials known to possess this characteristic, such is not the case for structural,

engineering systems. In the present work, an amorphous thermoplastic has been identified that non-autonomously heals at ~50°C after through penetration by a 224 mm diameter bullet at 900 m/sec. The objective of this study is to process the thermoplastic as matrix in a continuous CFRP and, determine the damage tolerance of the material in comparison to reported values for thermosetting, toughened epoxy CFRP.

### **1.1 Self-Healing Composites State-of-the-Art**

Self-healing thermoset polymeric materials are reported in the literature to mitigate incipient damage and have built-in capability to substantially recover structural load transferring ability after damage. In recent years, researchers have studied different “self-healing mechanisms” in materials as a collection of irreversible thermodynamic paths, where the path sequences ultimately lead to crack closure or resealing. Crack repair in polymers using thermal and solvent processes, where the healing process is triggered with heating or with a solvent, has been studied [3]. A second approach involves the autonomic healing concept, where healing is accomplished by dispersing a microencapsulated healing agent and a catalytic chemical trigger within an epoxy resin to repair or bond crack faces and mitigate further crack propagation [4]. A related approach, the microvascular concept, utilizes brittle hollow glass fibers in contrast to microcapsules filled with epoxy hardener and uncured resin in alternating layers [5-8]. An approaching crack ruptures a hollow glass fiber, releasing healing agent into the crack plane through capillary action. A third approach utilizes a polymer that can reversibly re-establish its broken bonds at the molecular level by either thermal activation (e.g., based on Diels-Alder rebonding), or ultraviolet light [9-12]. Various chemistries have been investigated based on the approaches described above. Although, significant recovery (>90%) of virgin neat resin material properties have been reported, this is not the case for fiber reinforced composites made from them. A fourth approach, the topic of this study, involves the integration of healing thermoplastic polymers as the resin matrix in a CFRP composite which heal quickly upon introduction of an external stimulus such as elevated temperature. A thermoplastic that demonstrated healing after through-penetration by a projectile, may possess the molecular structure to heal the matrix microcracks associated with low-velocity impact damage events before the microcracks accumulate and result in delamination.

The polymer self-healing approaches found in the literature have the following disadvantages: (1.) Slow rates of healing, (2.) Use of foreign inserts in the polymer matrix that may have detrimental effects on pristine composite performance, (3.) Samples have to be held in intimate contact or under load and/or fused together under high temperature for long periods of time, and/or (4). not considered a structural, load bearing material even in the pristine state. For example, a self healing composite that possesses aerospace quality consolidation with fiber volume fraction (FVF)≈60% and void volume fraction (VVF) < 2% does not currently exist [13]. Most self-healing composite laminates that have been reported possess 20-30% fiber volume, results in carbon fiber reinforced polymer (CFRP) composites with stiffness-to-weight ratios well below that required to replace aluminum in aerospace structure.

### **1.2 Advantages Offered by Composite with Puncture-Self-Healing Polymer Matrix**

Self-healing thermoplastic materials produce a matrix healing response from a change in the material's chain mobility as a function of the damage mechanism/condition involved. This type of material possesses non-autonomous healing capability at elevated temperatures, fast healing rates (less than 100 microseconds), and healing without the assistance of foreign inserts or fillers. Therefore, these materials have potential as structural aerospace materials.

Structures utilizing a self-healing thermoplastic matrix may provide the following advantages: 1) improved damage tolerance compared to industry SOA thermoset CFRP, 2) a route for recovery of a large proportion of the pristine mechanical properties, thus extending the life of the structure, 3) the potential to be directly substituted for conventional thermosetting matrices that do not possess self-healing characteristics, since conventional thermoset matrix composites already suffer a knockdown of up to 50% due to inherently low damage tolerance, and 4) repeated healing from multiple damage events as long as there is no loss of matrix material incurred in the event.

Neat resin plaques of the amorphous thermoplastic polybutadiene graft copolymer (PBg), shown in Figure 1, have been demonstrated to non-autonomously heal at 50°C after through penetration by a 224 mm projectile. A CFRP fabricated with any matrix that is penetrated by a projectile can never fully heal due to the presence of broken carbon fibers. However, a CFRP possessing a non-autonomous healing thermoplastic can recover a significant amount of compressive strength when healed after low velocity impact. The objectives of this study are to determine a) the mechanical performance of a CFRP fabricated using a non-autonomous healing thermoplastic matrix, b) the degree of recovery of pristine mechanical properties after impact damage is incurred, and c) conditions including heat and/or clamping force required to non-autonomously heal the matrix damage to maximize the recovery of pristine mechanical properties.

The PBg thermoplastic was selected for investigation as a matrix in carbon fiber reinforced polymer (CFRP) experimental composite due to its higher mechanical and thermal properties compared to the other self-healing thermoplastics which have been studied. According to material suppliers, PBg has a glass transition temperature,  $T_g = 80^\circ\text{C}$ , room temperature (RT) tensile strength of 37 MPa, RT tensile modulus of 2.47 GPa, and a 7.5% elongation at break[14]. The tensile modulus of the neat polymer is ~10% lower than the 2.76 GPa required of matrix polymers typically used in aerospace primary structural applications [15].

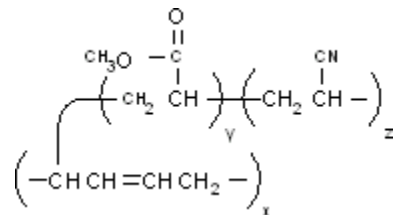


Figure 1. Chemical structure of the polybutadiene graft copolymer (PBg).

## 2. EXPERIMENTAL

### 2.1 Materials

The self-healing thermoplastic PB-co-g-PMA-co-PAN (PBg) pellets were obtained from Sigma-Aldrich®. Initially CFRP processing attempts with the PBg thermoplastic were conducted using woven carbon fabric IM7-6K 5-harness satin woven fabric (GP sizing, 280 gsm) from Textile Products, Inc., Anaheim, CA, USA. Experimental batches of PBg prepreg were developed using IM7-12K unsized fiber tow from ICI-Fiberite Inc. and anhydrous N-Methylpyrrolidone (NMP) solvent supplied by BASF® Chemical Co, Florham Park, New Jersey. Quasi-isotropic panels were fabricated for the purpose of consolidation quality comparison using Cycom® IM7/977-3 prepreg supplied by Cytec Engineered Materials, Woodland Park, New Jersey

### 2.2 Thermal Characterization

As a first step in determining the CFRP processing temperature window, the glass transition ( $T_g$ ) of the PBg polymer pellets were verified by conducting a dynamic temperature scan in nitrogen from 25°C to 300°C at 5°C/min in a Netzsch 204-F1 Phoenix® differential scanning calorimeter (DSC). In addition to the dynamic scan in DSC, dynamic temperature scans in nitrogen from 25°C to 300°C at 5°C/min were conducted using a Netzsch TG-209-F1 Libra® thermogravimetric analyzer (TGA) to determine the decomposition temperature of the pristine PBg polymer.

Residual solvent content in IM7/PBg prepreg, was determined from end roll specimens of the LaRC prepreg batch, designated tape machine run # (TM-341). A dynamic temperature scan in a Thermogravimetric Analyzer (TGA) under a nitrogen purge from 25°C to 300°C at 5°C/min was performed using a Netszsch TG-209-F1 Libra® TGA. This data was also used to determine the temperature which would be required to remove the volatiles (NMP) from the IM7/PBg prepreg during CFRP processing. These results were used to select an isothermal dwell temperature in the CFRP processing cycle prior to the compaction step, the time duration of this proposed dwell was determined by performing an isothermal scan at 150°C and 225°C in TGA of the IM7/PBg prepreg. Using a specimen from the TM341 roll of IM7/pB<sub>g</sub> prepreg, the mass evolution of the material during the proposed CFRP process cycle was determined in the Netzsch TGA by heating to 150°C at 5°C/min and holding for one hour under nitrogen purge and then heating from 150°C to the mold compaction temperature of 225°C at 5°C/min and holding for two hours.

### 2.3 Rheological Characterization

The PBg polymer was molded into neat resin disks 2.54 cm in diameter by 1.5 mm in thickness for rheological characterization in a Rheometrics ARESV® parallel plate rheometer. All of the rheology results presented in this study were collected using a cyclic strain of 2%. A dynamic temperature scan in nitrogen was conducted from 25°C to 285°C at 5°C/min. Based on the results of the TGA thermogram, an isothermal temperature scan at 150°C and 225°C was performed on the solution of NMP containing 31% solids PBg to determine the change in the dynamic viscosity as the matrix material devolatilizes during the proposed processing cycle.

## 2.4 Composite Process Development

PB<sub>g</sub> polymer pellets were dissolved in anhydrous NMP by continuously stirring for 48 hours at 25°C under nitrogen purge. The resulting uniform mixture contained 31% solids in NMP by weight. The Brookfield viscosity of the resulting solution at 25°C was determined to be 21.12 Pa\*sec (211.20 poise). This was acceptable for the solution prepregging process at LaRC. Two experimental batches of PB<sub>g</sub> prepreg were fabricated with LaRC prepregging equipment [16] over the course of this study. The 22 to 25 cm wide preps were processed using 90 unsized IM7-12K tows by introducing the PB<sub>g</sub>-NMP polymer in solution to the unsized IM7 fiber via the dip tank in the prepregging process. Using an established procedure [14] of weighing, oven drying, and reweighing samples of the prepreg, the resulting fiber areal weight (FAW), PB<sub>g</sub> resin and NMP solvent content of these two experimental batches were determined.

The processing cycle determined following the above tests and described in Section 3.3 was then used to fabricate three [45/0/-45/90]<sub>4S</sub> IM7/PB<sub>g</sub> panels including geometries of 7.6 cm x 7.6 cm, 15.2 cm x 15.2 cm, and 30.5 cm x 30.5 cm. Material from the first prepreg batch was processed in stainless steel closed molds using a TMP® 3 ton vacuum press with a layer of breather and release cloth separating the stack of prepreg from the stainless steel mold base and plunger. For the purpose of comparison in microscopy, a 15.2 cm x 15.2 cm [45/0/-45/90]<sub>4S</sub> panel was fabricated in the same mold and vacuum press using Cycom® IM7/977-3 toughened epoxy prepreg and the Cytec recommended processing cycle, C-49. Both the IM7/PB<sub>g</sub> and the IM7/977-3 15.2 cm x 15.2 cm panels were cross-sectioned at the panel center using a wet saw and then potted and polished for optical microscopy in a Reichert® MEF4 M microscope. Following ASTM D3171 [15], FVF/VVF analysis by acid digestion were conducted for this IM7/PB<sub>g</sub> panel and three subsequently processed 15.2 cm x 15.2 cm IM7/PB<sub>g</sub> panels. Based on these results, six additional [45/0/-45/90]<sub>4S</sub> 15.2cm x 15.2cm IM7/PB<sub>g</sub> panels were fabricated from prepreg batch (TM-340) and six from prepreg batch (TM-341) in the vacuum press for the purpose of determining the compression after impact (CAI) strength of these composite materials after low velocity impact damage.

## 2.5 Mechanical Property Characterization

Nine IM7/PB<sub>g</sub> panels were prepared as test coupons and subjected to low-velocity impact according to ASTM D7136 [16]. A spherical tup was used to impact each 15.2 cm x 10.1 cm coupon at the center. The average coupon thickness of the six panels fabricated from prepreg batch TM340 was 5.40 mm, and an impact energy of 36.08 J was used to damage these coupons. The six panels fabricated from prepreg batch TM-341 had an average thickness of 4.62 mm. Four of these six panels were damaged using an impact energy of 31.09 J. Non-destructive evaluation (NDE) by thru-transmission, time-of-flight c-scan of these impacted panels was conducted using a Sonotek® c-scan with a 10MHz transducer. After c-scan of all of the damaged coupons, one of the coupons from the panels fabricated using the TM-340 prepreg batch and three of those fabricated using the TM-341 batch were randomly selected and subjected to an elevated temperature/pressure healing cycle in the vacuum press using the following cycle:

25°C to 225°C at 5°C/min under full vacuum, hold at 225°C for 30 minutes under full vacuum and 1.7MPa pressure and cool down to 25C at 5°C/min under full vacuum.

Both pristine and damaged IM7/PB<sub>g</sub> quasi-isotropic laminates were tested according to ASTM D7137 [17] using a CAI test fixture in an MTS 250KN Load Frame. In addition, the pristine compression strength of the IM7/ PB<sub>g</sub> was determined by mounting these pristine 15.2 cm x 10.1 cm coupons in the CAI fixture and loading them in axial compression.

### 3. RESULTS AND DISCUSSION

#### 3.1 Thermal Characterization

The T<sub>g</sub> of the polymer was determined at the inflection in the heat vs temperature curve shown in Figure 2. This measured value of 75°C is very close to the vendor specified value of 80°C. A significant reduction in the modulus of the polymer is associated with this transition. For example, the tensile modulus of the PB<sub>g</sub> polymer at 25°C of 2.5 GPa is reduced to 2.2 MPa at 100°C as reported by the material supplier [25].

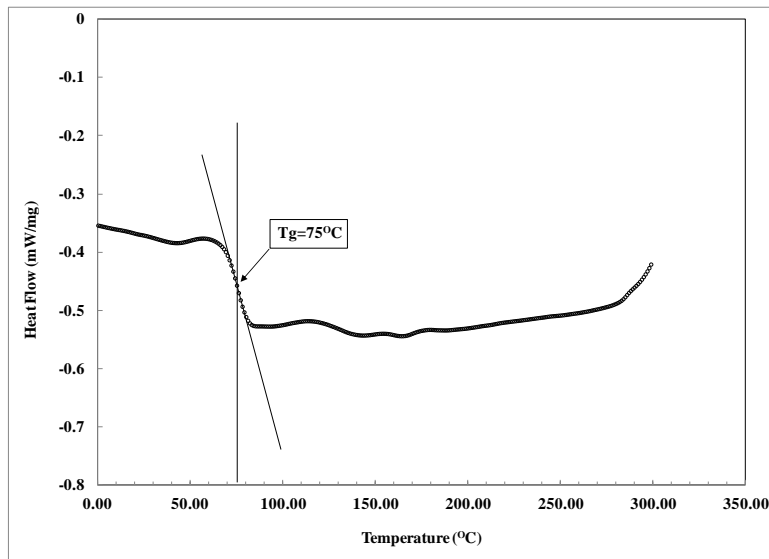


Figure 2. DSC Scan of pristine PB<sub>g</sub> amorphous thermoplastic.

The results of the dynamic temperature scan in TGA shown in Figure 3 indicates a pristine PB<sub>g</sub> sample mass loss of 2% at 300°C as the decomposition temperature and indicates that the polymer can be processed at temperatures up to 300°C without significant degradation.

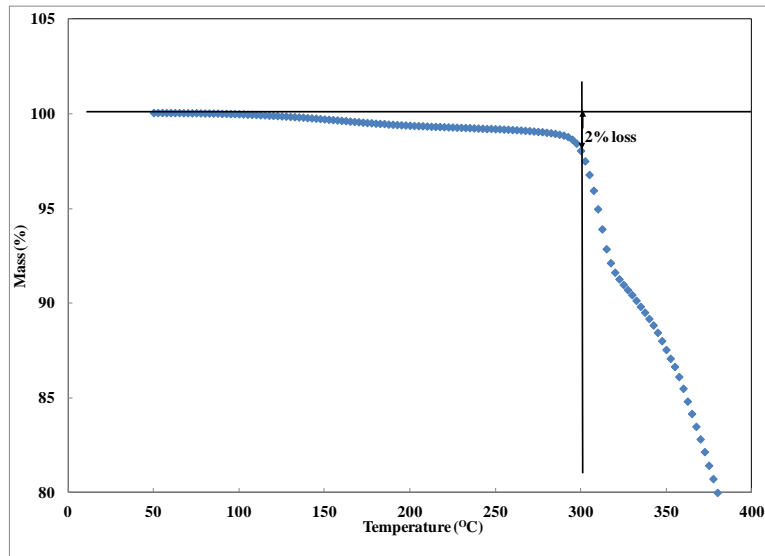


Figure 3. Dynamic temperature TGA of pristine PBg amorphous thermoplastic.

Residual solvent trapped in the prepreg will result in composite parts with high void content. The thermogravimetric scan shown in Figure 4 indicates that approximately 7% solvent evolved from the prepreg between 100°C and 200°C.

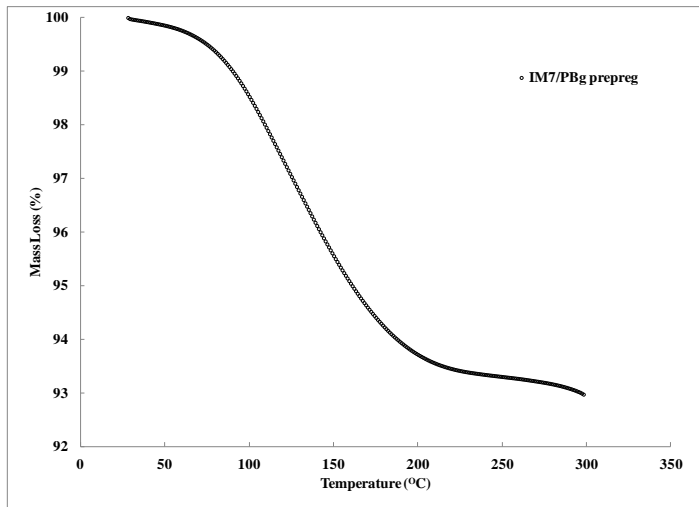


Figure 4. Mass evolution in dynamic temperature TGA scan of IM7/PBg prepreg containing NMP solvent.

Using these results, an isothermal dwell temperature of 150°C in the CFRP processing cycle was initially selected to devolatilize the IM7/PBg prepreg prior to the compaction step at 225°C. The temperature of 150°C also coincides with the reduced viscosity determined by rheological analysis. The time required in the proposed devolatilization dwell was investigated by isothermal TGA of the IM7/PBg prepreg. Shown below in Figure 5 are the mass evolution of both the pristine PBg polymer from pellet and the IM7/PBg prepreg during the proposed one hour isothermal drying step at 150 °C, as well as the two hour compaction step at 225 °C. The

isothermal TGA scans in Figure 5 indicate a mass loss of 1% in the pristine PBg polymer after one hour hold at 150°C, while the IM7/PB<sub>g</sub> prepreg lost up to 5% mass. This indicates a net devolatilization of NMP solvent of approximately 4% leaving a possible residual 6% (w) solvent in the prepreg, based on the total amount of solvent left in the prepreg after the prepegging process, going into the temperature ramp to the compaction and consolidation step at 225 °C. This level of solvent content could result in void entrapment during the compaction phase. The high viscosity of the PB<sub>g</sub> polymer might prevent the full removal of NMP, regardless of the devolatilization step duration. This will be a focus of future study.

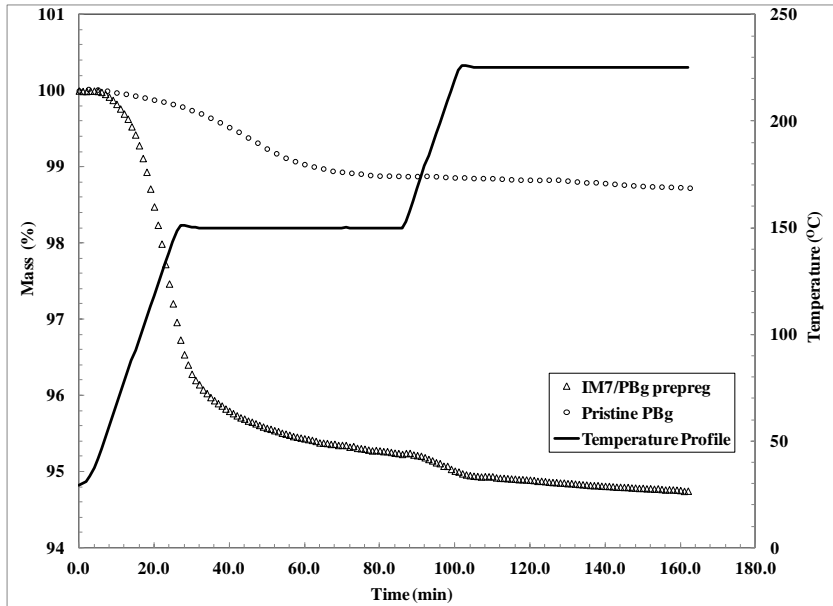


Figure 5. Isothermal mass evolution of pristine PB<sub>g</sub> and IM7/PB<sub>g</sub> prepreg.

### 3.2 Rheological Characterization

Having determined the T<sub>g</sub> and the decomposition temperature of the PB<sub>g</sub> polymer, the CFRP processing temperature window exists between 75°C and 300°C. Thermoplastic polymers are typically difficult to process as matrix in CFRP because the long molecular chains of these polymers make the bulk material highly viscous. Knowing the thermal processing window, the dynamic viscosity vs. temperature of the PB<sub>g</sub> polymer was determined via parallel plate rheology. The dynamic-temperature rheology scan in Figure 6 indicates that the PB<sub>g</sub> polymer exhibits two separate events where the heat introduced to the material results in significant reduction of the dynamic viscosity,  $\eta^*$ . Following the stick-slip phenomenon in the first 20 minutes of the test, the first event occurs near 150°C where the dynamic viscosity decreased from a maximum of 5,000 Pa\*sec (50,000 poise) to 1,500 Pa\*sec (15,000 poise). The second event occurs near 260°C where the PB<sub>g</sub> polymer reaches its minimum dynamic viscosity of 360 Pa\*sec (3,600 poise). However, the rapid increase in the viscosity at temperatures above 275°C, combined with the 2% mass loss observed in TGA indicates that the polymer is beginning to degrade at this elevated temperature. Therefore a maximum molding temperature of 225°C with

viscosity of 1,300 Pa\*sec (13,000 poise) was selected to process the PBg as matrix in CFRP composites.

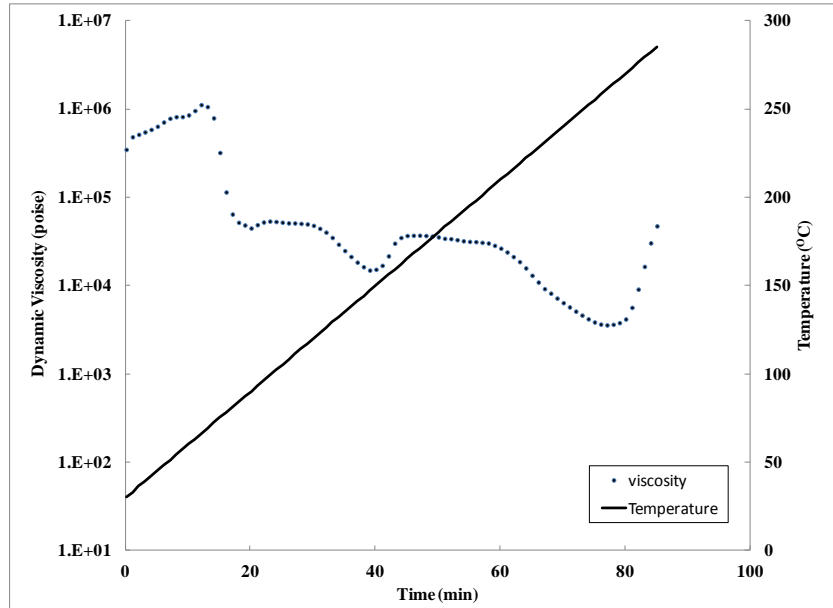


Figure 6. Dynamic temperature viscosity profile of the pristine PBg thermoplastic.

After determining the mass evolution in TGA of the IM7/PBg prepreg during the proposed CFRP processing devolatilization step at 150°C and compaction step at 225°C, the effect of these processing dwells on the dynamic viscosity of the PBg polymer was investigated in parallel plate rheology. The results of this isothermal temperature scan performed using the PBg-NMP prepping solution are shown below in Figure 7. During the isothermal hold at 150°C the PBg containing residual NMP exhibited a relatively stable viscosity of 1,500Pa\*sec (15,000) poise. A significant decrease in dynamic viscosity was observed during the 5°C/min temperature ramp to 225°C. During the 60 min hold at 225°C, the viscosity of the material was less stable, increasing from 6,700 poise at the beginning to 12,300 poise by the end of the isothermal hold. The change in viscosity may be due to devolatilization of the NMP solvent, which has a boiling point of 200°C at atmospheric pressure or the increase may be due to some initial degradation of the PBg molecule.

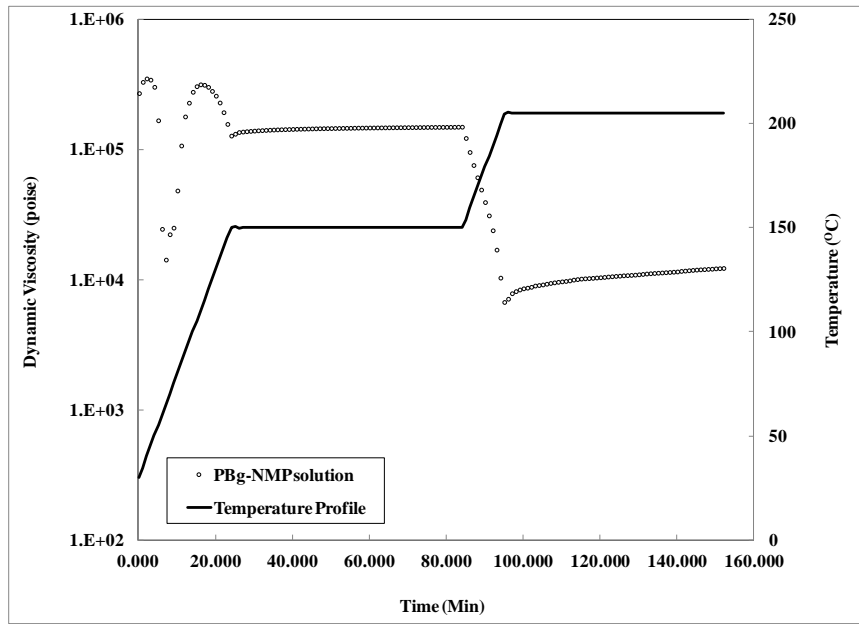


Figure 7. Isothermal temperature, dynamic viscosity of PBg- NMP solution.

### 3.3 Composite Process Development

The resin film infusion (RFI) process is preferable to alternative methods that require an intermediate step of pre-impregnating carbon fiber tows with resin. However, the photomicrograph in Figure 8 shows that this method was not suitable for PBg.

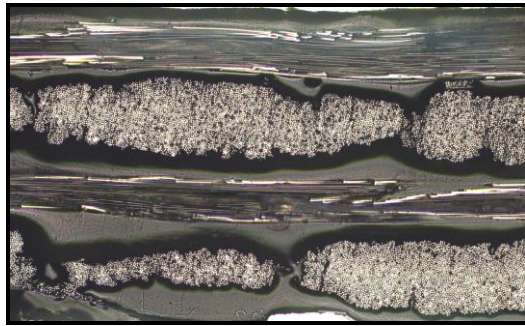


Figure 8. Photo-microscopy at 50X of IM7 5-harness satin biaxial/PBg matrix composite by RFI.

It is noted that the PBg resin was able to flow around the IM7-6K fiber tows in the biaxial fabric, but does not penetrate the tows. In fact the tows which are 90° to the plane are clearly surrounded by a region of voids. Based on these results, the effort to fabricate CFRP with PBg thermoplastic matrix focused on the development of a processing method with an intermediate prepreg material.

Two experimental batches of PBg prepreg were fabricated over the course of this study using prepregging equipment available in the LaRC Advanced Composites Processing Laboratory. The fiber areal weight (FAW), PBg resin and NMP solvent content of these two experimental batches are displayed in Table 1.

Table 1. Characteristics of NASA LaRC IM7/PB<sub>g</sub> unidirectional prepeg.

Run Number	Resin Viscosity, Poise	FAW, g/m <sup>2</sup>	Resin Content, wt% Dry	Solvent Content, wt% Wet	Width, cm	Length, m
TM-340	210	159	41-43	15-20	25	66
TM-341	211	146-150	34-35	10-11	22	59

Based on the results obtained in the thermal and rheological analysis of the IM7/PB<sub>g</sub> experimental prepeg, the processing cycle in the vacuum press for the IM7/PB<sub>g</sub> composite was selected to be:

1. 25°C to 150°C at 2°C/min under full vacuum, hold at 150°C under full vacuum for 60 minutes,
2. 150°C to 225°C at 2C/min under full vacuum, hold at 225°C for 60 minutes under full vacuum and 1.7MPa compaction pressure during entire temperature hold,
3. Cool down to 25°C at 2°C/min under full vacuum.

Using these conditions, three [45/0/-45/90]<sub>4S</sub> panels measuring 7.6 cm x 7.6 cm, 15.2 cm x 15.2 cm, and 30.5 cm x 30.5 cm were fabricated. Upon visual inspection, all three of these panels exhibited higher consolidation quality than the previous RFI panels. Both the IM7/PB<sub>g</sub> and the IM7/977-3 15.2 cm x 15.2 cm panels were cross-sectioned at the center using a wet saw and then potted and polished for photo microscopy. The resulting images are shown side-by-side for comparison below in Figure 9.

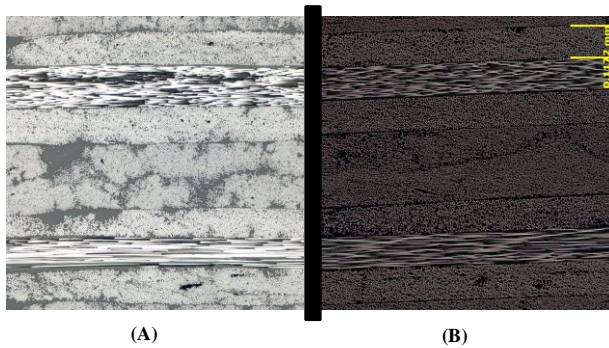


Figure 9. Optical micrographs at 100X of (A) IM7/PB<sub>g</sub> and (B) IM7/977-3.

The micrographs in Figure 9 of the center plies of the 32-ply quasi panels indicate that the IM7/977-3 composite was very well consolidated and essentially void free, or consistent with VVF <2%. The plies had uniform thickness of 0.127 mm and the fibers were uniformly dispersed with the epoxy matrix in each of the plies. The micrograph of the IM7/PB<sub>g</sub> composite at the same stack location show that the plies were fairly uniform with average thickness of 0.183 mm, but there were some resin fiber discontinuities, or resin-rich regions. There were several small voids evident in this small sampling of the overall composite. Photomicrographs of additional IM7/PB<sub>g</sub> composites fabricated at LaRC over the course of this study also contained

voids, especially near panel edges. These were likely formed by the NMP volatiles trapped in the highly viscous polymer. Void content analysis by acid digestion, using a polymer density of 1.31 g/cc, of three subsequent 32 ply quasi-isotropic 15.2 cm x 15.2 cm IM7/PB<sub>g</sub> panels revealed an average FVF > 60%, and average VVF < 2%. Based on these results, additional IM7/PB<sub>g</sub> panels from both experimental batches of prepreg were fabricated in the vacuum press for the purpose of determining the compression after impact (CAI) strength of these novel composite materials.

### 3.4 Mechanical Property Characterization

Nine IM7/PB<sub>g</sub> panels were subjected to low-velocity impact resulting in an average damage dent depth of 1.9 mm (0.075 in). The damage regions of all the impacted coupons were analyzed by c-scan. A representative image of the damage incurred in the IM7/PB<sub>g</sub> panels is shown in Figure 10a. NDE of these IM7/PB<sub>g</sub> coupons indicated an average planar delamination area of 15.3 cm<sup>2</sup>. The damage area and dent depth are consistent with barely visible impact damage (BVID).

Four of the BVID IM7/PB<sub>g</sub> panels were subjected to an elevated temperature/pressure healing cycle described above in the Experimental Section 2.5 and then tested to failure in compression to determine the influence of the cycle on the IM7/PB<sub>g</sub> composite CAI failure strength.

The time-of-flight c-scan image of one of these IM7/PB<sub>g</sub> panels before, (A), and after, (B), healing is shown in Figure 10. As a result of the elevated temperature/pressure healing cycle, no apparent damage was evident in the c-scan. After the healing cycle, the 1.9 mm deep dent on the surface of the panel was no longer visible.

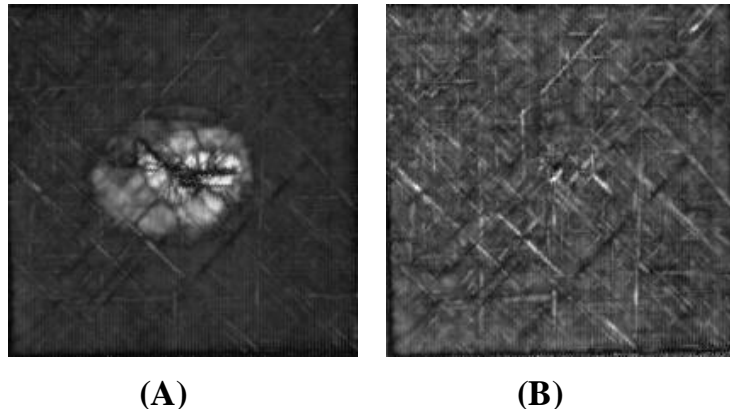


Figure 10. Thru transmission c-scan of IM7/PB<sub>g</sub> panel post impact:(A) and post-impact, post-healing cycle:(B).

The results of the axial compression of the two pristine IM7/PB<sub>g</sub> coupons, the five BVID coupons and the four BVID coupons subjected to an elevated temperature/pressure healing cycle are shown in Figure 11.

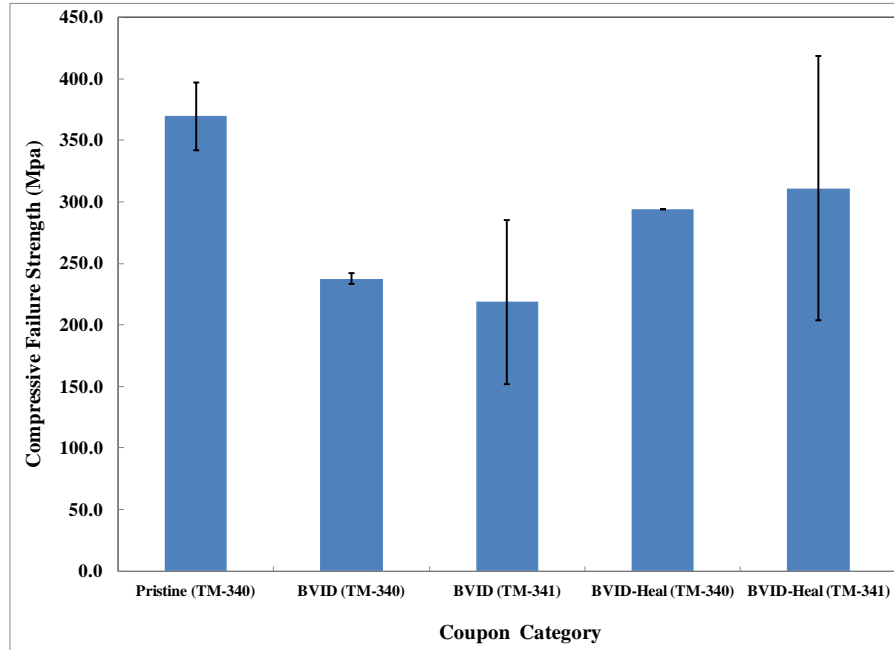


Figure 11. IM7/PB<sub>g</sub> testing results of pristine coupon compression, BVID coupon CAI and BVID-Healed coupon compression prepared from two batches of experimental prepreg (TM340) and (TM341).

All of the coupons failed due to fiber micro-buckling. In the five BVID coupons, this failure initiated at the site of the impact damage and propagated across the width of the coupons. The four IM7/PB<sub>g</sub> coupons containing BVID which were subjected to an elevated temperature/pressure healing cycle also failed due to fiber microbuckling initiating at the original impact site and propagating across the 10.2 cm width of the coupons. The pristine compressive strength resulting from this limited sample of coupons of quasi-isotropic laminates was approximately 52% of the compressive strength of the 675MPa reported [20] for a typical toughened epoxy 32-ply quasi-isotropic CFRP intended for aerospace structure.

The CAI strength of the BVID coupons appears to be independent of the prepreg batch. This is expected since the failure of these coupons is dominated by the impact damage and in this study the impact energy used for BVID was varied to account for the panel thickness variation resulting from prepreg batch inconsistency. The inconsistency of the prepreg batches was not of significant concern at this initial phase in the study given that all of the LaRC IM7/PB<sub>g</sub> prepreg were considered experimental. The differences in the batch to batch quality is noted in Table 1 and demonstrates that there is considerable room for improvement in both the quality of the prepreg and the resulting mechanical performance of CFRP panels fabricated from the intermediate material. In addition to the inconsistencies in the experimental prepreg, the fiber/matrix interface is not optimized with fiber sizing used to optimize the interfacial adhesion in toughened epoxy CFRPs. Compatible fiber sizing will be a focus of study to improve the mechanical performance of future carbon fiber/PB<sub>g</sub> composites.

Regardless of prepreg batch, there was a significant improvement in the failure strength of the BVID coupons subjected to an elevated temperature/pressure non-autonomous healing cycle vs

the BVID panels which were not healed. The TM340 batch of damaged IM7/PB<sub>g</sub> panels exhibited a 64% retention of compressive strength. The retention of compressive strength of coupons fabricated from this same batch of prepreg, which were subjected to BVID and then the elevated temperature/pressure healing cycle was found to be 80%. However, the large error associated with the BVID-Heal coupons from the second prepreg batch (B2) indicates that this notable improvement in compressive strength may be just as dependent on the quality of the CFRP laminate as it is on the non-autonomous healing capability of the matrix. The non-autonomic healing cycle utilized in this initial study amounts to reprocessing of the amorphous thermoplastic PB<sub>g</sub> matrix in the IM7/PB<sub>g</sub> composite. Unfortunately, the elevated temperature heating cycle and the high compaction pressure used during this healing cycle are not considered practical for in-flight, or even in-service grounded repair of aerospace vehicles. However, recovery of compression properties following the non-autonomic healing suggests the potential for a more damage tolerant structural composite if optimal processing conditions can be realized.

#### 4. CONCLUSIONS

In summary, a commercially available puncture-self-healing thermoplastic was previously identified in ballistic through-penetration impact testing of molded neat resin plaques. The PB-co-g-PMA-co-PAN (PB<sub>g</sub>) supplied by Sigma Aldrich was selected to be investigated as a possible CFRP matrix material to improve composite laminate damage tolerance. IM7/PB<sub>g</sub> CFRP composites were successfully fabricated by consolidating laminates made using solution processed prepreg. Two small experimental batches of experimental IM7/ PB<sub>g</sub> prepreg were produced in-house, possessing differing FAW. Based on thermal and rheological characterization of the prepreg material, a process cycle was developed to fabricate panels up to 30.5 cm x 30.5 cm. Optical microscopy and acid digestion analysis of a small population of these panels revealed favorable consolidation quality. Several [45/0/-45/90]<sub>4S</sub> laminates were fabricated from both of the LaRC IM7/PB<sub>g</sub> experimental batches of prepreg and utilized to characterize the CAI strength of the IM7/PB<sub>g</sub> CFRP. Four of the BVID IM7/PB<sub>g</sub> coupons were subjected to a non-autonomic healing cycle at elevated temperature/pressure, similar in heat and pressure magnitude to the developed composite processing cycle. C-scan of these coupons both before and after the healing cycle indicates that the delaminations at the impact site had been non-autonomously healed or, at least, were no longer visible. Compression testing of these healed coupons demonstrated significant improvement in retention of strength compared to coupons having BVID. These preliminary results suggest there is potential for using PB<sub>g</sub> in structural composites to mitigate low velocity impact damage following optimization of the fiber/matrix interface. Non-autonomic self-healing repair of these composites can also be improved by optimizing the polymer's flow properties, while retaining its desirable mechanical properties. Such improvements are currently under investigation.

#### 5. REFERENCES

1. Kelly, L.G, "Composite Structure Repair," AGARD Report No 716, AFRL, Wright Patterson Air Force Base, 1983.
2. Wu,D.Y., Muere, S., and D. Solomon, "Self-Healing Polymeric Materials: A Review of Recent Developments," *Progress in Polymer Science*, 2008, 35, 479-522.
3. Wool, R.P., *Polymer Interfaces: Structure and Strength* (Hanser/Gardner, Munich, 1995).

4. White, S.R., Sotto, N.R., Geubelle, P.H., Moore, J.S., Kessler, M.R., Sriram, S.R., Brown, E.N., Viswanathan, S., *Nature*, 2001, 409, 794-797.
5. Pang, J.W., Bond, I.P, *Composites Part A: Applied Science and Manufacturing*, 2005, 36(2), 183-188.
6. Pang, J.W., Bond, I.P., *Composites Science and Technology*, 2005, 65 (11-12), 1791-1799.
7. Dry, C., *Int. J Mod Phys B*, 1992; 6(15-16), 2763-2771.
8. Dry, C., McMillan W., *Smart Mater Struct*, 1996, 5(3), 297-300.
9. John, M., Li, G., *Smart Mater Struct*, 2010, 19,075013-075024.
10. Nji, J., Li, G., *Smart Mater Struct*, 2010, 19, 035007-035015.
11. Chen, X., Dam, M., Ono, K., Mal, A., Shen, H., Nutt, S., Hera, *Science*, 2002, 295, 1698-1702.
12. Chen, X., Dam, M., Ono, K., Mal, A., Shen, H., Nutt, S., Hera, *Science*, 2002, 295, 1698-1702.
13. Varley, R.J., van der Zwaag, S., *Polym Int*, 2010, 59, 1031–1038.
14. Supplier Website: [http://www.ineosbarex.com/files/upload/Barex210Film\\_07\\_11.pdf](http://www.ineosbarex.com/files/upload/Barex210Film_07_11.pdf)
15. St.Clair, T.L., Johnston, N.J., ands R.M.Baucom, "High Performance Composites Research at NASA Langley," NASA TM 100518, 1988.
16. Cano, Roberto J, Johnston, N. J. and Marchello,J:, 40th SAMPE Symposium and Exhibition, Anaheim, CA, May, 1995.
17. ASTM Standard D3171-09 (2009), American Society for Testing and Materials, West Conshohocken, Pennsylvania (first issued in 1973).
18. ASTM Standard D7136-07 (2007), American Society for Testing and Materials, West Conshohocken, Pennsylvania (first issued in 2005).
19. ASTM Standard D7137-07 (2007), American Society for Testing and Materials, West Conshohocken, Pennsylvania (first issued in 2005).
20. Soutis, C and Lee, J., "A Study on the Compressive strength of Thick Carbon fiber-Epoxy Laminates," Composite Science and Technology, Volume 67 (10), 2007, pp 2016-2026.